Proc. Natl. Acad. Sci. USA
Vol. 92, pp. 2273–2277, March 1995
Plant Biology

Xanthophyll cycle-dependent quenching of photosystem II chlorophyll a fluorescence: Formation of a quenching complex with a short fluorescence lifetime

(picosecond time-resolved fluorescence/antheraxanthin/zeaxanthin/nonphotochemical fluorescence quenching)

ADAM M. GILMORE*, THEODORE L. HAZLETT†, AND GOVINDJEE*‡

*Department of Plant Biology, University of Illinois at Urbana-Champaign, 505 S. Goodwin Avenue, 265 Morrill Hall, Urbana, IL 61801; and †Laboratory for Fluorescence Dynamics, Department of Physics, University of Illinois, Urbana, IL 61801

Communicated by Olle Björkman, Carnegie Institution of Washington, Washington, DC, December 13, 1994

ABSTRACT **Excess light triggers protective nonradiative dissipation of excitation energy in photosystem II through the formation of a trans-thylakoid pH gradient that in turn stimulates formation of zeaxanthin and antheraxanthin. These xanthophylls when combined with protonation of antenna pigment–protein complexes may increase nonradiative dissipation and, thus, quench chlorophyll a fluorescence. Here we measured, in parallel, the chlorophyll a fluorescence lifetime and intensity to understand the mechanism of this process. Increasing the xanthophyll concentration in the presence of a pH gradient (quenched conditions) decreases the fractional intensity of a fluorescence lifetime component centered at ≈2 ns and increases a component at ≈0.4 ns. Uncoupling the pH gradient (unquenched conditions) eliminates the 0.4-ns component. Changes in the xanthophyll concentration do not significantly affect the fluorescence lifetimes in either the quenched or unquenched sample conditions. However, there are differences in fluorescence lifetimes between the quenched and unquenched states that are due to pH-related, but nonxanthophyll-related, processes. Quenching of the maximal fluorescence intensity correlates with both the xanthophyll concentration and the fractional intensity of the 0.4-ns component. The unchanged fluorescence lifetimes and the proportional quenching of the maximal and dark-level fluorescence intensities indicate that the xanthophylls act on antenna, not reaction center processes. Further, the fluorescence quenching is interpreted as the combined effect of the pH gradient and xanthophyll concentration, resulting in the formation of a quenching complex with a short (≈0.4 ns) fluorescence lifetime.**

A conserved mechanism protects photosystem II (PSII) in higher plants against damage by excess absorbed excitation energy (1, 2). It has been suggested that excess excitation of the PSII antenna is nonradiatively dissipated, causing nonphotochemical quenching (NPQ) of PSII chlorophyll (Chl) a fluorescence (Fig. 1) (1–4). Excess light triggers NPQ by first causing chloroplast lumen acidification. Proton pumping from either light-driven electron flow or the chloroplast ATPase can induce NPQ (3). Lumen acidity serves at least two roles in the NPQ mechanism. First it activates the xanthophyll cycle deepoxidase (5) that catalyzes violaxanthin (Vx) deepoxidation to zeaxanthin (Zx) via antheraxanthin (Ax) (6). Second, protonation apparently alters the conformation of PSII antenna and/or reaction center pigment–protein complexes, promoting interaction with the xanthophylls and somehow causing NPQ (3, 4, 7). In isolated chloroplasts, NPQ depends on both lumen acidification and Zx plus Ax (4). Uncouplers of the proton gradient reverse NPQ and inhibit deepoxidation (3–5).

The publication costs of this article were defrayed in part by page charge payment. This article must therefore be hereby marked "*advertisement*" in accordance with 18 U.S.C. §1734 solely to indicate this fact.

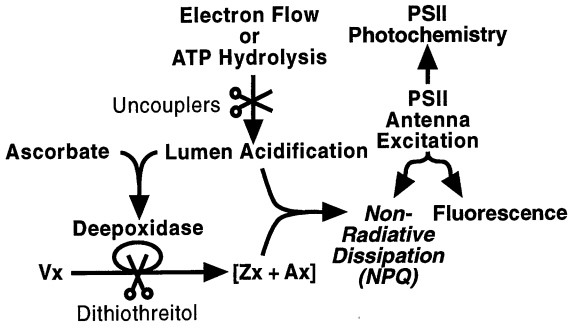

FIG. 1. Schematic summary of the light- and ATP-induced xanthophyll-dependent NPQ mechanism in isolated chloroplasts. Vx, violaxanthin; Zx, zeaxanthin; Ax, antheraxanthin

Dithiothreitol (DTT) inhibits deepoxidation but not lumen acidification (8) or NPQ caused by preformed Zx plus Ax (3, 4).

One proposed NPQ mechanism includes a role for Vx in preventing or reversing pH-dependent aggregation of PSII light-harvesting antenna complexes (LHCIIs) (9). Here, decreasing the Vx concentration, which is equivalent to increasing the sum of the Zx and Ax concentrations, [Zx + Ax] (Fig. 1), enhances LHCII aggregation and hence NPQ by creating weakly fluorescent long-wavelength-absorbing chlorophylls. However, Vx deepoxidation apparently does not induce long-wavelength-absorbing chlorophylls in leaves (10), and there is no indication of long-wavelength chlorophylls in other chloroplast studies (11, 12). Another suggested NPQ mechanism involves the trans-thylakoid pH gradient (ΔpH) causing Ca^{2+} release from and inhibition of the PSII donor side (13); thus, due to PSII donor side inhibition, the quinone acceptor of PSII (Q_A) remains oxidized and photochemically quenches Chl a fluorescence.

The processes competing for the de-excitation of the excited state determine the quantum yield of fluorescence—i.e., $\phi_F = k_f/(k_f + k_p + k_t + k_n)$, where k_f is the rate constant of Chl a fluorescence, k_p is the rate constant of photochemical quenching by oxidized Q_A, k_t is the rate constant of energy transfer

Abbreviations: Ax, antheraxanthin; *c*, center of fluorescence lifetime distribution; Chl, chlorophyll; DCMU, 3-(3,4-dichlorophenyl)-1,1-dimethylurea; DTT, dithiothreitol; *f*, fractional intensity of fluorescence lifetime or distribution; F_m (F'_m), maximal fluorescence intensity in the absence (presence) of NPQ; F_o (F'_o), minimal fluorescence intensity in the absence (presence) of NPQ; LHCP (LHCII), light-harvesting pigment–protein complex (of PSII); NPQ, nonphotochemical quenching of PSII Chl a fluorescence; PAM, pulse-amplitude modulation fluorimeter; PSII, photosystem II; Q_A, primary quinone electron acceptor of PSII; Vx, violaxanthin; Zx, zeaxanthin; ΔpH, trans-thylakoid proton gradient; $\langle\tau\rangle(\langle\tau\rangle')$, average lifetime of Chl a fluorescence in the absence (presence) of NPQ; *w*, width at half maximum of fluorescence lifetime distribution.

‡To whom reprint requests should be addressed.

from fluorescent PSII to weakly fluorescent photosystem I, and k_n is the rate constant of nonradiative dissipation. NPQ is thus presumably determined by k_n, which is apparently proportional to the lumen proton concentration and [Zx + Ax] (4). However, current kinetic models cannot be used to interpret available data and determine whether NPQ occurs in the PSII antenna or reaction center complexes (for a review, see ref. 14). On the one hand, the kinetic model of Butler and Kitajima (15) predicts that increasing k_n in the PSII antenna should quench both the minimal (F_o; maximum k_p) and maximal (F_m; $k_p = 0$) fluorescence intensity; quenching that affects charge separation in the reaction center should not affect F_o. On the other hand, the exciton radical pair equilibrium model (16) for PSII suggests that the reaction center P680 Chl a is a shallow trap and that charge recombination of the radical pair can allow an exciton to diffuse back to the antenna. Therefore, the exciton radical pair model, which assumes PSII photochemistry is trap-limited, contrasts with Butler and Kitajima's model (15), which assumes that exciton diffusion from the antenna to the reaction center limits charge separation. Thus, in the exciton radical pair model, F_m and F_o quenching by NPQ could be proportional to each other in either the reaction center or antenna complexes, but quenching of F_m and *not* F_o indicates an effect on charge separation (14). Several reports show that NPQ of F_o is proportional to that of F_m (3, 9, 17), in contrast to a report by Krieger *et al.* (13), which shows no F_o quenching.

In this paper we compared, in parallel, the xanthophyll concentration, the Chl fluorescence lifetimes, and the quenching of F_m and F_o to gain insight into the NPQ mechanism. Analyses of the fluorescence lifetimes clearly show that NPQ is due to a xanthophyll-dependent increase in the fractional intensity of a specific Chl a component with a short fluorescence lifetime. The lifetime data suggest that NPQ is due to the formation of a xanthophyll-dependent quenching complex. The lifetime and intensity (F_m and F_o) data together indicate that NPQ differs mechanistically from Q_A quenching. The results are discussed in terms of the current biophysical and structural models of PSII fluorescence and xanthophyll-induced NPQ.

MATERIALS AND METHODS

Time-Resolved Chl a Fluorescence Measurements. Fluorescence lifetimes were measured with a multifrequency cross-correlation fluorimeter (model K2; ISS Instruments, Urbana, IL) (18–20). Sample excitation at 610 nm was provided by a cavity-dumped rhodamine 6G dye laser (Coherent, Palo Alto, CA) pumped by a mode-locked Nd:YAG laser (Coherent). The sample was excited under "magic-angle" (54.7°) conditions. Data were collected at 16 separate sinusoidally modulated excitation frequencies ranging from 7 to 300 MHz. The frequencies were mixed randomly during acquisition to minimize systematic errors from sample bleaching. Emission at wavelengths >620 nm was monitored through a red Hoya R-64 cutoff filter. The shift in phase angles (phase) and demodulation ratios (modulation) of the sample fluorescence emission were analyzed for fluorescence lifetime information. Further details and explanation of the multifrequency cross-correlation technique can be found elsewhere (18–20). The fluorescence lifetime data are presented as the lifetimes (τ) and fractional intensities ($f_i = \alpha_i\tau_i/\Sigma\alpha_i\tau_i$, where α_i is the preexponential amplitude factor representing the fractional contribution of the component with the lifetime τ_i). Plots of Lorentzian lifetime distributions were normalized to a value of 1 for the major component.

Chloroplast Isolation. Fresh spinach (*Spinacia oleracea*) and lettuce (*Lactuca sativa* L. cv. Romaine) leaves were obtained locally and stored at least 12 h (dark, 4°C) before chloroplast isolation (3). The chloroplasts were osmotically shocked (10–15 s) in 1 ml of distilled water and then brought to 5 ml and 30 μM Chl a + b in a reaction medium containing 50 μM methylviologen, 0.3 mM ATP, 0.1 M sucrose, 10 mM NaCl, 10 mM KCl, 5 mM $MgCl_2$, 10 mM Tricine, 1 mM KH_2PO_4, and 0.2% (wt/vol) defatted bovine serum albumin adjusted to pH 8.0 with NaOH. This procedure yielded the thylakoid membranes used in this study.

Experimental Protocol. Fig. 2 shows an example, using spinach thylakoids, of the Chl fluorescence intensity determinations with the pulse-amplitude modulation fluorimeter (PAM) (model 103; Heinz Walz, Effeltrich, F.R.G.) (21). We measured F_o (minimum fluorescence) with a <0.15 μmol of photons per m^2 per s (1.6 kHz) beam and F_m (maximum fluorescence) with a 2-s light pulse (5000 μmol of photons per m^2 per s after passing through a Heinz Walz model DT-cyan filter). The white continuous actinic light (450–500 μmol of photons per m^2 per s; Corning CS1-75 infrared filter) was turned on as the PAM measuring beam was switched to 100 kHz. After a 15-min light exposure, 3 mM DTT was added to stop deepoxidation (Fig. 1) and to assure thiol activation of the ATPase (22). The minimal fluorescence intensity in the presence of NPQ (F'_o) was monitored 1 min after turning off the continuous light, and then the sample was transferred to dark at 0°C. The sample, now in a "quenched" condition as far as the Chl a fluorescence is concerned, was prepared for the lifetime measurements by diluting a portion to a final volume of 3 ml and 7.5 μM Chl a + b; all other reagents were the same as in the reaction mixture except that 3-(3,4-dichlorophenyl)-1,1-dimethylurea (DCMU; 10 μM) was added. The quenched sample was analyzed in the lifetime instrument at 5°C within ≈15 min. Then, as shown in Fig. 2*B*, the sample was rapidly placed in the PAM where the quenched maximal fluorescence intensity in the presence of NPQ (F'_m) was measured, the ΔpH was uncoupled with nigericin, and the "unquenched" F_m was determined. The unquenched fluorescence lifetime data were either immediately taken, or the samples were stored (dark, 0°C) until the quenched samples were finished; neither the lifetimes nor F_m changed during ice storage (<4 h).

The [Zx + Ax] was controlled by the DTT concentration added before illumination [i.e., 3 mM for complete inhibition and usually <0.25 mM for subsaturating inhibition (4)]. The high [Zx + Ax] was obtained by omitting DTT during the first 15 min of actinic illumination, and the low [Zx + Ax] samples had 3 mM DTT before illumination. We restricted changes in fluorescence during the lifetime measurements to changes in nonradiative dissipation by adding DCMU, which eliminates photochemical quenching by inhibiting Q_A^- oxidation, and methylviologen, which inhibits energy transfer changes (23). Under these conditions, the ATPase ΔpH remained very constant for >0.5 h.

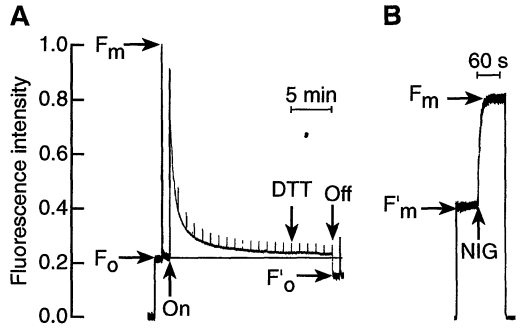

FIG. 2. Chl a fluorescence intensity determinations in spinach thylakoids for F_m, F'_m, F_o, and F'_o. The final unquenched F_m was measured 60 s after adding 2 μM nigericin (NIG). The sample cuvette for the PAM was at 15°C. Similar results were obtained with lettuce thylakoids. "On" and "Off" refer to turning the continuous actinic light on and off, respectively.

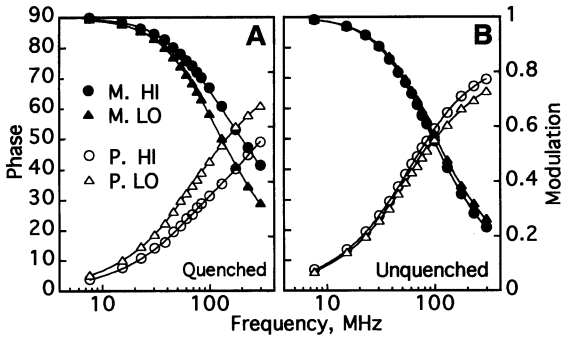

FIG. 3. Frequency dependence of phase (P) and modulation (M) data for spinach thylakoids under conditions of quenched (*A*) and unquenched (*B*) Chl a fluorescence. HI and LO refer to 31 and 10 mmol of Zx + Ax per mol of Chl a + b, respectively. The smooth curves represent the best double-Lorentzian fits through the data points.

A 1.5-ml aliquot from each original sample (30 μM Chl a + b) was treated with 2 μM nigericin and saved at −80°C for HPLC pigment analysis (24).

RESULTS

Xanthophyll Quenching and the Lorentzian Lifetime Distributions of Chl a Fluorescence. It is now established that proteins exist in a distribution of structurally slightly different conformational substates (25). Because Chl molecules are always bound in a protein complex and their excited states should be sensitive to their environment, we expect the excited states of Chl to show a distribution of lifetimes corresponding to the distribution of conformational substates of the pigment–protein complex, as already observed (19, 20). The excited state heterogeneity of Chl a should be better represented by a continuous Lorentzian distribution as opposed to a discrete set of exponential decays. The phase and modulation data for spinach thylakoids with 10 (LO) and 31 (HI) mmol of Zx plus Ax per mol of Chl a + b and the best fit to bimodal Lorentzian decays for both the quenched (with NPQ) and unquenched conditions are shown in Fig. 3 *A* and *B*, respectively. Under quenched conditions and with increasing frequencies, low [Zx + Ax] correlated with higher phase shift and lower modulation compared to high [Zx + Ax] (Fig. 3*A*). This indicated a decrease in the mean sample lifetime with increasing [Zx + Ax]. The unquenched samples (Fig. 3*B*), however, had similar phase shift and modulation, showing that [Zx + Ax] exerts little or no effect on them.

Fig. 4 shows that the Lorentzian lifetime distributions were bimodal in spinach thylakoids when quenched with 31 (Fig. 4*A*) or 10 mmol Zx plus Ax per mol of Chl a + b (Fig. 4*C*). In the quenched samples, the increased [Zx + Ax] raised the fractional intensity of the shorter (≈0.4 ns) lifetime component (compare *A* with *C* in Fig. 4). The longer lifetime component, centered around 2 ns (Fig. 4 *A* and *C*), appears to be analogous to the unquenched component at ≈2.4 ns (Fig. 4 *B* and *D*).

Table 1 shows the average lifetime centers (c_1 and c_2), widths (w_1 and w_2), and fractional intensities (f_1 and f_2) from bimodal Lorentzian distribution analyses of all available spinach and

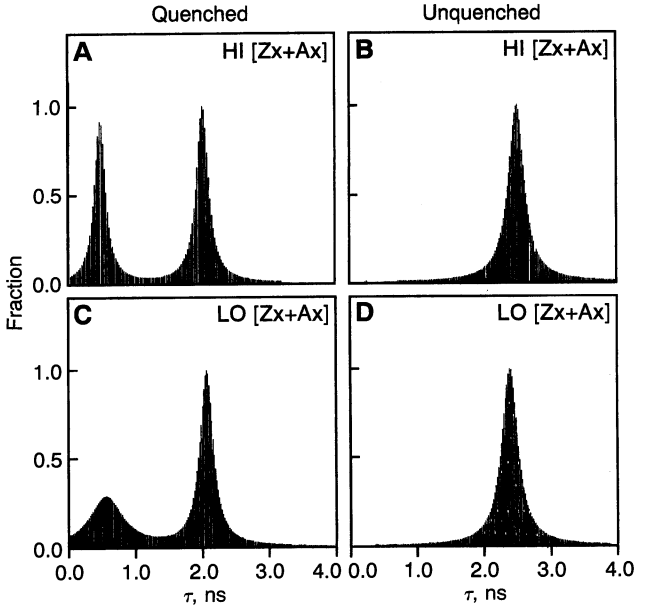

FIG. 4. Plots of Lorentzian lifetime distributions for spinach thylakoids with quenched and unquenched Chl a fluorescence in the presence of both high (HI; 31 mmol Zx + Ax) and low (LO; 10 mmol of Zx + Ax) xanthophyll concentrations. χ^2 = 2.078 for *A*, 1.085 for *B*, 1.249 for *C*, and 1.393 for *D*.

lettuce samples and with quenched or unquenched Chl fluorescence. A slight decrease in the longer (c_1) lifetime component in the quenched, compared to unquenched, samples was independent of the [Zx + Ax]. This lifetime decrease could have been due to pH-induced changes in the antenna protein conformation. Further, the w_1 components were, on the average, narrowed under the quenched conditions. We interpret this to mean that the protein conformational environment of these Chl fluorescence components is more homogeneous under quenched conditions. In contrast to w_1, the w_2 component is broadened during quenching, suggesting a more heterogeneous environment for that component.

Although the values for c_1 and c_2 are constant and independent of [Zx + Ax] during quenching, f_1 and f_2 under quenched conditions vary with changes in [Zx + Ax] (Fig. 5, Table 1). Fig. 5*A* shows that the conversion between these fractional intensities [i.e., the f_1 (2 ns) component to the f_2 (0.4 ns) component] correlates with $(F_m/F'_m) - 1$ in both spinach and lettuce thylakoids. Fig. 5*B* shows that [Zx + Ax] correlates with $(F_m/F'_m) - 1$, in agreement with our earlier report (4). There is an apparent threshold level for both the f_2 component (Fig. 5*A*) and [Zx + Ax] (Fig. 5*B*) before $(F_m/F'_m) - 1$ is measurable under quenched conditions.

Discrete Exponential Decay and Average Lifetime Analysis. For a comparison with the above Lorentzian analyses, Table 2 shows the fits of spinach and lettuce data to a triple-exponential decay model. Tabulated are the discrete lifetimes and fractional intensities, which together determine the average lifetime, $\langle\tau\rangle$. Four samples were analyzed—namely, those unquenched and quenched with high [Zx + Ax] and un-

Table 1. Lorentzian *c*, *w*, and *f* for conditions of quenched and unquenched Chl fluorescence in spinach and lettuce thylakoids

Sample	Chl fluorescence	c_1, ns	w_1, ns	f_1	c_2, ns	w_2, ns	f_2
Spinach	Quenched	1.90 ± 0.08	0.22 ± 0.06	Variable*	0.42 ± 0.06	0.50 ± 0.11	Variable*
Spinach	Unquenched	2.25 ± 0.05	0.42 ± 0.07	0.92 ± 0.02	0.40 ± 0.07	0.28 ± 0.12	0.08 ± 0.02
Lettuce	Quenched	2.14 ± 0.07	0.25 ± 0.06	Variable*	0.34 ± 0.09	0.31 ± 0.05	Variable*
Lettuce	Unquenched	2.36 ± 0.03	0.48 ± 0.06	0.91 ± 0.02	0.50 ± 0.18	0.13 ± 0.05	0.09 ± 0.02

This analysis was made by using a bimodal Lorentzian distribution model. All values are the means ± SE, and n = 10 for both spinach and lettuce.
*The variations in f_1 and f_2 that were caused by changes in [Zx + Ax] under quenched conditions are plotted against $(F_m/F'_m) - 1$ in Fig. 5*A*.

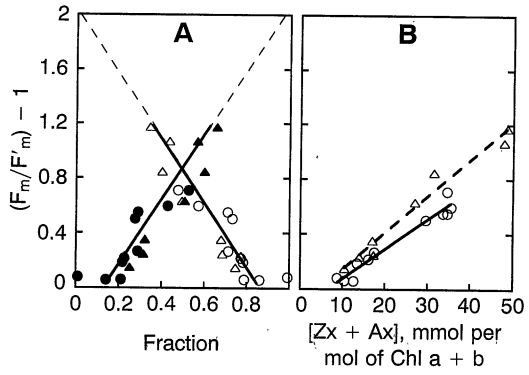

FIG. 5. Relationship between $(F_m/F'_m) - 1$ and the Lorentzian fractional intensities (*A*) and the [Zx + Ax] (*B*). (*A*) Solid symbols indicate the quenched f_2 values in Table 1 of spinach (▲) and lettuce (●) thylakoids, respectively. Open symbols indicate the quenched f_1 values in Table 1. (*B*) The plots were fit by linear regression, and the r^2 values for spinach (△) and lettuce (○) were 0.969 and 0.956, respectively. For spinach and lettuce the [Vx + Ax + Zx] were 83 ± 6 and 82 ± 3 mmol per mol of Chl a + b, respectively.

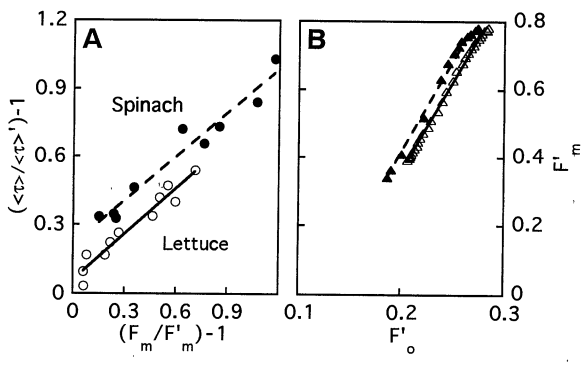

FIG. 6. (*A*) Relationship between $(\langle\tau\rangle/\langle\tau\rangle') - 1$ and $(F_m/F'_m) - 1$ for spinach and lettuce thylakoids. The $\langle\tau\rangle$ and $\langle\tau\rangle'$ values were calculated for each point as in Table 2. The equations of the regression lines for spinach and lettuce were $(\langle\tau\rangle/\langle\tau\rangle') - 1 = 0.64(F_m/F'_m - 1) + 0.21$; $r^2 = 0.96$ and $(\langle\tau\rangle/\langle\tau\rangle') - 1 = 0.67(F_m/F'_m - 1) + 0.06$; $r^2 = 0.94$, respectively. For spinach (and lettuce) ratios of variable fluorescence to maximal fluorescence (F_v/F_m) before light treatment were 0.79 ± 0.01 (and 0.80 ± 0.004). (*B*) Plots of F'_o against F'_m in lettuce chloroplasts at 30°C (△) and 25°C (▲). Both F'_o and F'_m are normalized relative to the preillumination F_m (see Fig. 2); the preillumination F_v/F_m was 0.785 for both samples. The [Zx + Ax] was 63 ± 4 mmol per mol of Chl a + b for both samples. The equations of the regression lines were $F'_o = 0.19F'_m + 0.13$; $r^2 = 0.997$ (30°C) and $F'_o = 0.19F'_m + 0.12$; $r^2 = 0.990$ (25°C).

quenched and quenched with low [Zx + Ax]. The low χ^2 values indicated a goodness of fit similar to the Lorentzian models (Fig. 4 legend). Also similar to the Lorentzian model, [Zx + Ax] had little or no significant effect on the fractional intensities and lifetimes in the unquenched samples (Table 2). Furthermore, in the quenched samples the major changes during quenching occurred in the fractional intensities (values in parentheses) and not the lifetimes. In contrast to the Lorentzian model, the discrete analysis showed larger lifetime changes between the quenched and unquenched samples along with fractional shifts in both the plant species. The quenched $\langle\tau\rangle'$ values (i.e., the average lifetime of Chl a fluorescence in the presence of NPQ) are clearly shorter in the high than in the low [Zx + Ax] samples, whereas the unquenched $\langle\tau\rangle$ values are independent of [Zx + Ax]. In Fig. 6*A* the slopes of the linear plots of $(F_m/F'_m) - 1$ against $(\langle\tau\rangle/\langle\tau\rangle') - 1$ were 0.64 and 0.67 for spinach and lettuce, respectively. Importantly, as with the Lorentzian model, these analyses show that the changes in measured F_m that are correlated with changes in $\langle\tau\rangle$ are mainly due to changes in the fractional intensities of the discrete exponential lifetime components.

Effects of NPQ on F_m and F_o. Fig. 6*B* shows F'_o plotted against F'_m for experiments with lettuce thylakoids similar to the experimental conditions used in Fig. 2*A*. Here, after a preillumination period where NPQ was induced, we recorded the values over a 1-h dark period during which the ATP-induced NPQ slowly and completely relaxed. DCMU was omitted from these samples to allow for complete Q_A^- oxidation between the high-intensity light flashes used for the F'_m measurements. The F'_o and F'_m showed a linear correlation with only a slight deviation at the high range of F'_m and F'_o. In short, these data established that F'_o and F'_m are quenched in a linear proportion to each other and confirmed that NPQ does not affect charge recombination in the reaction center.

DISCUSSION

Xanthophyll Cycle-Induced Quenching of Chl a Fluorescence. Increasing the Vx deepoxidation to Zx + Ax during NPQ correlates with the conversion of a 2-ns Lorentzian fluorescence lifetime component to a 0.4-ns component (Fig. 4 and Table 1); this conversion decreases the fluorescence yield and quenches F_m (Fig. 5). Because the fluorescence lifetimes of the Lorentzian distributions were independent of xanthophyll concentration during NPQ and also because the extent of NPQ is not inhibited at low temperatures (ref. 26; this study), we conclude that NPQ is not controlled by rates of diffusive collisions. We instead suggest that NPQ is due to the formation of quenching complexes. The shorter fluorescence lifetime of the c_2 compared to the c_1 component is consistent with a higher rate constant of nonradiative dissipation (k_n) for the c_2 component. The differences between the fluorescence lifetime parameters of the two components during the quenching process suggest that they arise from antenna complexes in either an unquenched (c_1) or quenched (c_2) conformation, respectively. Interestingly, the apparent changes in the con-

Table 2. Discrete lifetimes, given in ns, and fractional intensities (in parentheses) under conditions of quenched and unquenched Chl fluorescence in spinach and lettuce thylakoids with either high or low [Zx + Ax]

	Spinach				Lettuce			
	Quenched		Unquenched		Quenched		Unquenched	
	High*	Low*	High*	Low*	High†	Low†	High†	Low†
τ_1	4.35 (0.08)	3.05 (0.31)	4.55 (0.10)	6.49 (0.04)	3.21 (0.27)	2.72 (0.70)	2.99 (0.68)	2.99 (0.65)
τ_2	1.73 (0.53)	1.54 (0.58)	2.37 (0.85)	2.39 (0.86)	1.41 (0.56)	1.09 (0.26)	1.46 (0.28)	1.53 (0.30)
τ_3	0.40 (0.39)	0.29 (0.10)	0.31 (0.05)	0.41 (0.10)	0.17 (0.17)	0.00 (0.03)	0.00 (0.04)	0.04 (0.05)
$\langle\tau\rangle'$ or $\langle\tau\rangle$‡	1.41	1.88	2.50	2.35	1.67	2.20	2.45	2.41
χ^2	1.891	0.888	0.892	1.480	2.90	2.36	1.58	1.08

The analysis was made using a three-exponential decay model.
*The high and low [Zx + Ax] for spinach were 31 and 10 nmol per mol of Chl a + b, respectively.
†The high and low [Zx + Ax] for lettuce were 34 and 13 nmol per mol of Chl a + b, respectively.
‡$\langle\tau\rangle$ (unquenched) and $\langle\tau\rangle'$ (quenched) = $\Sigma f_i\tau_i$.

formational state of the c_1 component between the quenched and unquenched conditions may be related to the NPQ activation step involving protonation of antenna complexes that is required (7), along with the presence of [Zx + Ax], for NPQ (3).

Gilmore and Yamamoto (27) had suggested that either the deepoxidation of Vx to Zx plus Ax affects the thylakoid membrane properties to stoichiometrically increase the number of protonated antenna complexes (e.g., light-harvesting pigment–protein complexes, or LHCPs) or protonation increases the number of active binding sites for Zx and Ax on the LHCPs. In the latter case, which appears more consistent with this data set, the question arises as to what physical mechanism is used to quench Chl a fluorescence by the xanthophylls. Xanthophylls, like long-chain polyenes, possess low-lying singlet excited states (28), which in the cases of Zx and Ax lie below or at, respectively, the Q_Y absorption band of Chl a, allowing a downhill excitation energy transfer from Chl a to Zx or Ax. Perhaps a specific, pH-activated binding of the xanthophylls to an LHCP may facilitate this process.

Regarding a role for Vx deepoxidation in controlling LHCP protonation and/or LHCII aggregation (9), it remains to be determined whether increasing LHCII aggregation *in vivo* would result in the same pattern of change for the two Lorentzian components as observed in this study. Moreover, it must still be considered that NPQ may be due to other stoichiometric, but indirect, effects of both the lumen pH and [Zx + Ax] on the antenna proteins, which could affect the Lorentzian parameters of the Chl fluorescence components. In any case, NPQ under the experimental conditions of this study depended on the [Zx + Ax], which is different from the observations of Horton and co-workers (9, 29).

Differences Between Q_A Quenching and NPQ of Chl Fluorescence. The proportional quenching of both F_m and F_o (Fig. 6*B*) indicates that NPQ is independent of both charge separation and stabilization in the PSII reaction center (14, 16), since both should have been held constant by the presence of DCMU in our experiments. Additionally, photochemical fluorescence quenching by Q_A exerts its most significant effect on the lifetimes of the fluorescence components as opposed to the amplitudes (13); however, in this study the fluorescence lifetimes of the Lorentzian distributions were independent of [Zx + Ax] (Table 1 and Figs. 4 and 5). Moreover, in contrast to Krieger *et al.* (13), NPQ was not inhibited by ascorbate, itself needed for deepoxidation (5). Importantly, the lack of ascorbate inhibition and the presence of F_o quenching during NPQ confirmed Genty *et al.* (17), who also showed that NPQ in barley leaves correlated with a decrease in the fluorescence lifetimes of two components for F_m and one component for F_o. However, Genty *et al.* (17) did not have DCMU present during their NPQ lifetime measurements; thus, the role of Q_A quenching was not eliminated.

NPQ and Xanthophyll Cycle Localization. Regarding the NPQ site, the xanthophyll cycle pigments are reportedly associated exclusively with the CP24, CP26, and CP29 complexes of PSII (30). However, others (31, 32) have suggested that the xanthophylls distribute more evenly among the various LHCPs. In any case, it appears that the functional association of the xanthophylls with the proposed quenching complexes and thus with the NPQ process depends on the ΔpH. Interestingly, the xanthophyll cycle epoxidation reaction can competitively reverse NPQ in the presence of a ΔpH (33). Therefore, we conclude that the xanthophyll cycle pigments apparently function in NPQ to interconvert protonated antenna complexes between the 2-ns and 0.4-ns fluorescence components, thus modulating protective nonradiative dissipation in response to limitations to photosynthetic capacity.

We are grateful to Dr. Olle Björkman and Mrs. Connie Shih for their excellent HPLC pigment analysis. We thank Dr. Peter Debrunner for critically reading the manuscript. A United States Department of Energy/United States Department of Agriculture/National Science Foundation Integrated Photosynthesis Research Training Grant (IPTRG) postdoctoral fellowship to A.M.G. is gratefully acknowledged. G. was supported in part by National Science Foundation Grant 91-16838 (Supplement 1994).

1. Björkman, O. & Demmig-Adams, B. (1993) in *Ecological Studies*, eds. Schulze, E.-D. & Caldwell, M. (Springer, Berlin), Vol. 100, pp. 17–47.
2. Demmig-Adams, B. & Adams, W. W., III (1992) *Annu. Rev. Plant Physiol. Plant Mol. Biol.* **43,** 599–626.
3. Gilmore, A. M. & Yamamoto, H. Y. (1992) *Proc. Natl. Acad. Sci. USA* **89,** 1899–1903.
4. Gilmore, A. M. & Yamamoto, H. Y. (1993) *Photosynth. Res.* **35,** 67–78.
5. Hager, A. (1969) *Planta* **89,** 224–243.
6. Yamamoto, H. Y., Nakayama, T. O. M. & Chichester, C. O. (1962) *Arch. Biochem. Biophys.* **97,** 168–173.
7. Crofts, A. R. & Yerkes, C. T. (1994) *FEBS Lett.* **352,** 265–270.
8. Sokolove, P. M. & Marsho, T. V. (1976) *Biochim. Biophys. Acta* **430,** 321–326.
9. Horton, P., Ruban, A. V. & Walters, R. G. (1994) *Plant Physiol.* **106,** 415–420.
10. Bilger, W. & Björkman, O. (1994) *Planta* **193,** 238–246.
11. Yamamoto, H. Y., Kamite, L. & Wang, Y. Y. (1972) *Plant Physiol.* **49,** 224–228.
12. Pfündel, E. E. (1993) *Photochem. Photobiol.* **57,** 356–361.
13. Krieger, A., Moya, I. & Weis, A. (1992) *Biochim. Biophys. Acta* **1102,** 167–176.
14. Dau, H. (1994) *Photochem. Photobiol.* **60,** 1–23.
15. Butler, W. L. & Kitajima, M. (1975) *Biochim. Biophys. Acta* **376,** 116–125.
16. Schatz, G. H., Brock, H. & Holzwarth, A. R. (1988) *Biophys. J.* **54,** 397–405.
17. Genty, B., Goulas, Y., Dimon, B., Peltier, G., Briantais, J.-M. & Moya, I. (1992) in *Research in Photosynthesis*, ed. Murata, N. (Kluwer, Dordrecht, The Netherlands), Vol. 4, pp. 603–610.
18. Alcala, J. E., Gratton, E. & Prendergast, F. G. (1987) *Biophys. J.* **51,** 597–604.
19. Govindjee, Van De Ven, M., Preston, C., Seibert, M. & Gratton, E. (1990) *Biochim. Biophys. Acta* **1015,** 173–179.
20. Govindjee, Van De Ven, M., Cao, J., Royer, C. & Gratton, E. (1993) *Photochem. Photobiol.* **58,** 438–445.
21. Schreiber, U., Schliwa, U. & Bilger, W. (1986) *Photosynth. Res.* **10,** 51–62.
22. Petrack, B. & Lipman, F. (1961) in *Light and Life*, eds. McElroy, W. D. & Glass, B. (Johns Hopkins Press, Baltimore), pp. 621–630.
23. Horton, P. & Black, M. T. (1981) *Biochim. Biophys. Acta* **635,** 53–62.
24. Gilmore, A. M. & Yamamoto, H. Y. (1991) *J. Chromatogr.* **543,** 137–145.
25. Frauenfelder, H., Parak, F. & Young, R. D. (1988) *Annu. Rev. Biophys. Biophys. Chem.* **17,** 451–479.
26. Bilger, W. & Björkman, O. (1991) *Planta* **184,** 226–234.
27. Gilmore, A. M. & Yamamoto, H. Y. (1993) in *Photosynthetic Responses to the Environment*, eds. Yamamoto, H. Y. & Smith, C. M. (Am. Soc. Plant Physiol., Rockville, MD), pp. 160–165.
28. Frank, H. A., Cua, A., Chynwat, V., Young, A., Gostzola, D. & Wasielewski, M. R. (1994) *Photosynth. Res.* **41,** 389–395.
29. Mullineaux, C. W., Pascal, A. A., Horton, P. & Holzwarth, A. R. (1993) *Biochim. Biophys. Acta* **1141,** 23–28.
30. Bassi, R., Pineau, B., Dainese, P. & Marquardt, J. (1993) *Eur. J. Biochem.* **212,** 297–303.
31. Thayer, S. S. & Björkman, O. (1992) *Photosynth. Res.* **33,** 213–225.
32. Thornber, J. P. & Peter, G. F. (1991) *J. Biol. Chem.* **266,** 16745–16754.
33. Gilmore, A. M., Mohanty, N. & Yamamoto, H. Y. (1994) *FEBS Lett.* **350,** 271–274.